

Rationalization of incisor shape: Experimental-numerical analysis

Pascal Magne, Dr Med Dent,^a Antheunis Versluis, MS, PhD,^b and William H. Douglas, BDS, MS, PhD^c
School of Dentistry, University of Minnesota, Minneapolis, Minn., and School of Dental Medicine, University of Geneva, Geneva, Switzerland

Statement of problem. Moving from the posterior segment in the anterior direction within the dental arch, the process of “incisivation” takes place. The occlusal table is gradually replaced by an incisal edge that has the function of cutting.

Purpose. This study considers these genetically controlled changes by using strain gauge measurements and finite element analyses to rationalize the clinical and biologic advantages of incisal form. A direct clinical link in the common esthetic procedure of anterior veneering is expected.

Material and methods. Six maxillary incisors were mounted in a positioning device and equipped with 2 strain gauges bonded to the palatal surface: gauge 1 (G1) in the concavity and gauge 2 (G2) on the cingulum. A 50 N load was applied on the palatal side of the incisal edge, perpendicular to the long axis of the tooth. Displacement of the load tip and the palatal strain were recorded after successively removing one third, two thirds, and the total thickness of the facial enamel. The same experiment was reproduced with the finite element method (FEM). Four additional experimental designs were tested with the FEM by simulating the progressive thinning and elimination of palatal enamel and a thickened palatal lobe. Surface tangential stresses and local strain in the area corresponding to gauges 1 and 2 were calculated from the postprocessing files.

Results. The FEM was validated by experimental results considering both displacement of the load tip ($\sim 120 \pm 30 \mu\text{m}$) and tangential surface strain at G1/G2. Recorded strains were always higher in the concavity when compared with the cingulum; high tensile strains were recorded at G1 after the total removal of the facial enamel. The entire facial surface was submitted to compressive forces. Subsequent compressive stresses were higher ($\sim 150 \text{ MPa}$) when facial enamel was thin or when the palatal enamel was removed. However, their absolute value never reached the elevated and potentially harmful tensile stresses measured in the palatal concavity, especially in the absence of facial enamel (272 MPa). Multiple experimental cracks were generated in the remaining palatal enamel as a consequence of stress redistribution. However, smooth and convex surfaces with local enamel bulk such as the cingulum, the marginal ridges, and the facial cervical third of the anatomic crown showed the lowest stress level. The optimal configuration with regard to the stress pattern was given by the modified natural tooth that exhibited thick palatal enamel and a mostly convex palatal surface.

Conclusions. Palatal concavity that provides the incisor with its sharp incisal edge and cutting ability proved to be an area of stress concentration. This shortcoming can be compensated by specific areas that feature thick enamel such as the cingulum and the marginal ridges. When enamel is worn or removed from the facial surface, its replacement should be carried out by using materials with properties similar to enamel to restore the original biomechanical behavior of the tooth. (*J Prosthet Dent* 1999;81:345-55.)

CLINICAL IMPLICATIONS

The understanding of tooth hard tissues is essential to the development of restorative procedures. New trends in restorative dentistry consist of reproducing the original performances of the intact tooth (“biomimetics”). This study presents a theoretical description of stress distribution within intact incisors, which could set the reference for developments in restorative designs, for example, in the optimized techniques for the treatment of crown-fractured incisors.

This study was supported by the Swiss Science Foundation (Grant 81GE-50071) and in part by the Minnesota Dental Research Center for Biomaterials and Biomechanics.

^aVisiting Associate Professor, Minnesota Dental Research Center for Biomaterials and Biomechanics, Department of Oral Science, School of Dentistry, University of Minnesota; and Lecturer, Department of Prosthodontics and Department of Prevention and Therapeutics, School of Dental Medicine, University of Geneva.

^bAssistant Professor, Minnesota Dental Research Center for Biomaterials and Biomechanics, Department of Oral Science, School of Dentistry, University of Minnesota.

^cProfessor and Academic Director, Minnesota Dental Research Center for Biomaterials and Biomechanics, Department of Oral Science, School of Dentistry, University of Minnesota.

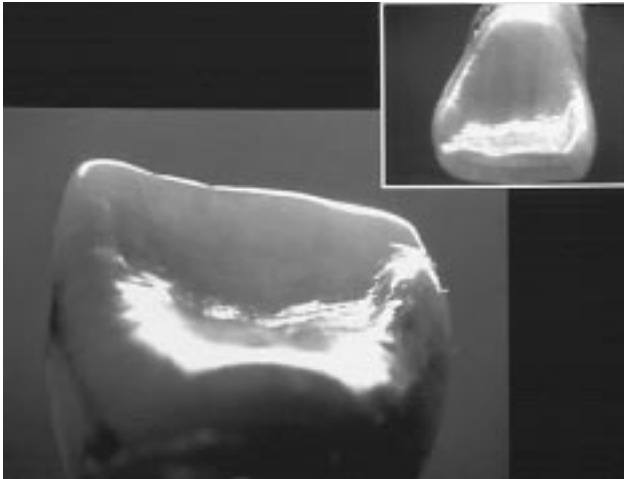


Fig. 1. Detailed views of intact maxillary central incisor, palatal surface. Prominent lateral ridges and cingulum define contour of palatal concavity.

Global understanding of the natural tooth with regard to its intrinsic structure, biology, and external shape is essential when restorative principles are discussed. For the problem of biomechanical response, posterior teeth have been the first focus of researchers with analysis of biophysical stress in molars and premolars.^{1,2} Even though anterior and posterior teeth display similar mechanical and physical properties, the geometric and functional loading configuration of incisors must be distinguished. Moving from the posterior segment in the anterior direction within the dental arch, the process of “incisivization” takes place, which means the occlusal table is gradually replaced by an incisal edge that has the function of cutting. From a biomechanical standpoint, it is important to discern the basic properties of enamel and dentin and the anatomic features of the teeth.

Enamel and dentin exhibit different basic physical properties. They form a “composite” structure that provides a tooth with unique characteristics³: The hardness of enamel protects the soft underlying dentin; however, the crack-arresting effect of dentin and of thick collagen fibers at the dentinoenamel junction (DEJ)⁴ compensate for the inherently brittle nature of enamel. This structural and physical interrelationship between an extremely hard tissue and a more pliable softer tissue provides the natural tooth with the unique ability to withstand high masticatory and thermal loads. Although multiple enamel cracks are usually encountered in aged teeth, these senile changes seldom affect the integrity of the enamel-dentin complex.

Anatomically, incisors show highly contrasting structure between facial and palatal surfaces. The labial aspect of the crown is mainly convex (enamel prisms

get larger toward the surface), whereas the palatal portion of the tooth displays a deep concavity that extends axially between the dental cingulum and the incisal edge and laterally between the 2 strong proximal ridges (Fig. 1). Because of this specific shape, the incisal edge is designed like a blade, which plays a major role in the cutting efficiency of the tooth. In some situations, the palatal concavity is interrupted by vertical lobes rising from the cingulum. The portion of the crown featuring the thinnest enamel layer, namely, the cervical third, is also the area of maximum underlying thickness of dentin. Inversely, the thick incisal enamel is supported by a thin dentin wall. Because of the arrangement and position of the anterior dentition, mechanical loads are mainly acting in the buccopalatal plane of each tooth. Mesiodistal loads are restrained by proximal contact areas.

Anterior esthetic techniques often involve labial and interproximal reduction of enamel, which makes the tooth crown more deformable.^{5,6} The resistance of the crown to deformation is a major contributor to the fracture strength of the tooth. The effect of varying levels of enamel reduction is quantitatively determined by the crown flexure, which can be measured under simulated conditions by bonded strain gauges. However, it is difficult to gain access to the intimate structure of the tooth-restoration complex with traditional experimental methods alone. Consequently, the finite element method (FEM) has become a well-accepted modeling tool⁷ and new trends in research tend to combine both experimental approach and FEM evaluation in the same investigation.^{6,8,9} In finite element analysis, a large structure is divided into a number of small simple-shaped elements for which individual deformation (strain and stress) can be calculated more easily than for the whole undivided large structure. By solving the deformation of all the small elements simultaneously, the deformation of the whole structure can be reconstructed.

The aim of this study was to describe the mechanical response of maxillary incisors in terms of surface stress and strain distribution based on experimental evaluations, along with FEM simulations. Special attention was given to the effect of tooth shape (concavities vs convexities) and composition (enamel-dentin distribution).

METHOD AND MATERIAL

Experimental strain gauge model

Six extracted maxillary central incisors were collected, scaled, and stored in saline solution and azide 0.2% at 4°C. Teeth were mounted in a special positioning device with a hard dental stone (Vel Mix Stone, Kerr Mfg, Orange, Calif.) by embedding the root up to 1.5 mm below the facial level of the cemento-enamel junction (CEJ) (Fig. 2). Two strain gauges (type CEA-

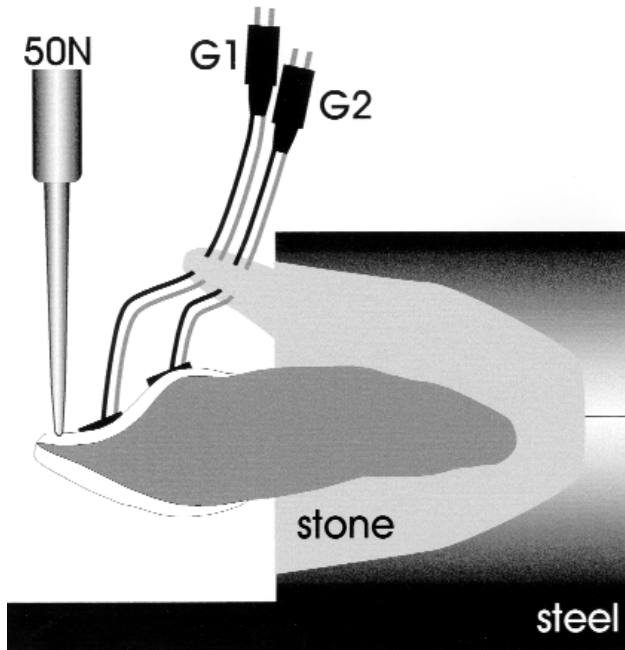


Fig. 2. Schematic representation (section) of tooth specimen embedded in stone and positioned for load test. Gauge G1 is placed in palatal concavity and gauge G2 on cingulum.

06-032UW-120, Measurements Group Inc, Raleigh, N.C.) were bonded to each specimen, one in the palatal concavity (G1) and the other on the cingulum (G2) of the anatomic crown, following the longitudinal axis of the tooth (Fig. 3). Each test specimen was wired in half of a Wheatstone bridge circuit, along with an intact reference tooth to use the common mode rejection. A small depression was created 1 mm from the incisal edge and centered mesiodistally on the palatal surface. This allowed a standardized positioning for load application in a closed-loop servohydraulic universal testing machine (MTS Systems, Eden Prairie, Minn.). Loading was applied perpendicular to the long axis of the tooth, in the direction of the facial surface.

A realistic biting load can be separated into horizontal and vertical components. The horizontal component induces bending and would be the major challenge for the incisor. The force was controlled with a digital function generator to allow a ramp loading from 1 to 51 N in 8 seconds. Force/strain curves were generated, and the local compliance or flexibility (ratio between maximum strain and maximum load) at G1 and G2 was calculated. The measurement was repeated 5 times for each specimen and each experimental design. Recorded curves were linear and reproducible during the repeated runs. The maximum displacement of the load tip was also recorded with a mechanical dial indicator. Because the material properties of fully calcified tissue depend on hydration,^{10,11} the teeth were kept wet during the entire experiment.



Fig. 3. Detailed view of specimen after placement of strain gauges. Axis of gauges follows longitudinal axis of tooth. Load point is marked in red.

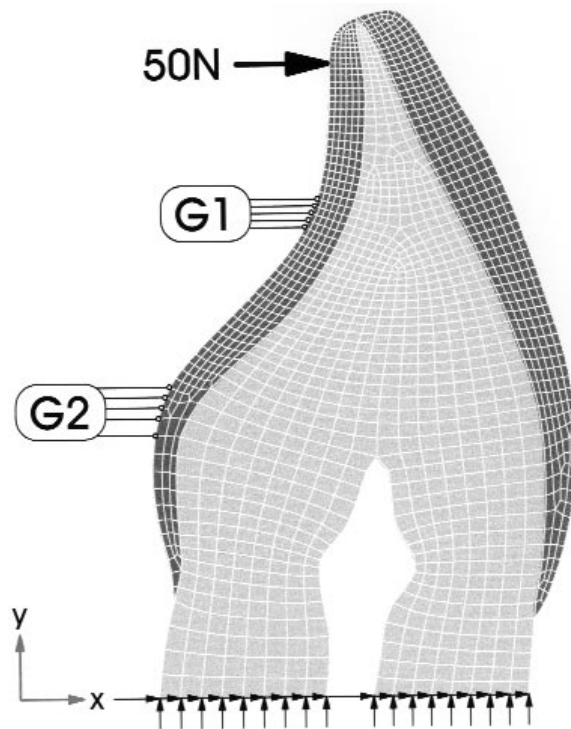


Fig. 4. Two-dimensional finite element model of natural tooth consisting of 1489 elements and 1589 nodes. Enamel shell was intentionally designed with 6 layers of elements, except for cervical section. This allowed successive removal of $\frac{1}{3}$ (2 layers), $\frac{2}{3}$ (4 layers), and full thickness of enamel. First row of nodes at cervical base of tooth were fixed in x- and y-axes.

Finite element model and analysis

An extracted maxillary central incisor was selected, embedded in a clear resin, and sectioned longitudinally in the buccolingual plane. The sectioned surface was

	<p>nat: <u>experimental</u> & FE intact original central incisor</p> <p>FE: 1489 elements / 1589 nodes</p>		<p>p1: <u>FE only</u> removal of 1/3 of the palatal enamel thickness.</p> <p>FE: 1390 elements / 1491 nodes</p>
	<p>f1: <u>experimental</u> & FE removal of 1/3 of the facial enamel thickness</p> <p>FE: 1374 elements / 1475 nodes</p>		<p>p2: <u>FE only</u> removal of 2/3 of the palatal enamel thickness.</p> <p>FE: 1296 elements / 1398 nodes</p>
	<p>f2: <u>experimental</u> & FE removal of 2/3 of the facial enamel thickness</p> <p>FE: 1252 elements / 1350 nodes</p>		<p>p3: <u>FE only</u> total removal of the palatal enamel</p> <p>FE: 1206 elements / 1308 nodes</p>
	<p>f3: <u>experimental</u> & FE total removal of the facial enamel</p> <p>FE: 1133 elements / 1230 nodes</p>		<p>natm: <u>FE only</u> original incisor modified with an additional palatal lobe</p> <p>FE: 1489 elements / 1589 nodes</p>

Fig. 5. Experimental conditions and finite element model definition.

digitized with a computer scanner (UMAX, Umax Data System Inc, Hsinchu, Taiwan). The contour of enamel, dentin, and pulp chamber were manually traced with graphic software (Freelance Graphics, Lotus, Cambridge, Mass.), and the lines were then transferred to a workstation (Silicon Graphics, Mountain View, Calif.) for the generation of a mesh by using Mentat software (MARC Analysis Research Co, Palo Alto, Calif.) (Fig. 4). The root was not modeled, as it may be assumed that the overall stress distribution in the coronal restoration is marginally affected by the root area under the simulated boundary conditions. The load in the finite element model was equivalent to the load for the experimental strain gauge model, namely, a point load of 50 N in the x direction on a palatal node 1 mm from the incisal edge. Fixed zero-displacement in both horizontal and vertical directions were applied at the cut-plane of the root. The stress distribution was solved with the MARC solver. Although teeth are 3-dimensional structures, a 2-dimensional finite element model with plane strain elements (linear, 4-node, isoparametric, arbitrary quadrilateral) was chosen because of its improved performances in terms of element number and simulation quality. Although more realistic, 3-dimensional models present coarser meshes that would not allow the fine representation of tooth form and thin layers. Moreover, the accuracy of 2-dimensional analysis considered in a

buccolingual cross-section has been demonstrated² and validated in a companion article¹ by experimental strain measurements. At least 2 mechanical material properties were required for this finite element simulation: the modulus of elasticity (Young's modulus) and Poisson's ratio. A variety of values are recorded in the literature. As reported by Versluis et al,¹² a correct ratio of moduli (enamel/dentin) is necessary for a qualitative linear analysis. Moduli of 50 and 12 GPa were chosen for enamel and dentin, respectively, yielding to a ratio of 4.2. Poisson's ratios of 0.23 for dentin¹³ and 0.30 for enamel¹⁴ were assumed.

Groups

Eight finite element models were generated from the same mesh: natural (nat), f1, f2, f3, p1, p2, p3, and modified natural (natm) conditions (Fig. 5). The respective influence of facial and palatal enamel on the surface stress distribution (condition nat vs f1-f3 and p1-p3) was evaluated by removing one third, two thirds, and the total enamel thicknesses, respectively. The full thickness of enamel was always maintained in the area of the load point. In the natm condition, the influence of enamel geometry and thickness was evaluated by changing the contour of the palatal surface. This specific design may feature the area of the proximal crest or an extended palatal tubercle. Because the strain gauges in the experimental model were placed on

$$\text{Relative compliance} = \frac{\text{Compliance at selected test condition}}{\text{Compliance given by the unaltered tooth}}$$

$$\text{Relative compliance} = \frac{\frac{\text{Maximum strain at selected test condition}}{\text{Maximum load}}}{\frac{\text{Maximum strain given by the unaltered tooth}}{\text{Maximum load}}}$$

$$\text{Relative compliance} = \frac{\text{Maximum strain at selected test condition}}{\text{Maximum strain given by the unaltered tooth}}$$

Fig. 6. Equation to give relative value to absolute measurements supplied by strain gauges.

the palatal surfaces, the 6 specimens were used essentially to test the conditions nat, f1, f2, and f3. The removal of facial enamel was controlled with silicone impression guides from the original tooth, as in clinical procedures.

Finite element postprocessing calculations

Finite element calculations generated the stress and strain values. Surface tangential stress, σ_t , for each node located at the outline of the tooth, was calculated from the values of stress in x and y directions (σ_x and σ_y) and xy-shear stress (τ_{xy}), by using the following transformation¹⁵:

$$\sigma_t = \frac{\sigma_x + \sigma_y}{2} + \frac{\sigma_x - \sigma_y}{2} \cos 2\theta + \tau_{xy} \sin 2\theta$$

where θ is the angle between x-axis and the surface of the element. Similarly, the surface tangential strain, ϵ_t , was calculated for the 10 nodes corresponding with the location of strain gauges in the experimental setup (5 nodes in G1 area, 5 nodes in G2 area) (Fig. 4) by using the values of strain in x and y directions (ϵ_x and ϵ_y) and xy-shear strain (ϵ_{xy}), integrated in the following transformation:

$$\epsilon_t = \frac{\epsilon_x + \epsilon_y}{2} + \frac{\epsilon_x - \epsilon_y}{2} \cos 2\theta + \frac{\epsilon_{xy}}{2} \sin 2\theta$$

RESULTS

Local compliance

Natural variations of teeth strongly affect absolute strain gauge measurements. Accordingly, for comparison among the specimens, normalized results were used. Absolute measurements supplied by the strain

Table I. Numerical results and standard errors

Specimen number	Experimental conditions	Relative compliance at G1	SD	Relative compliance at G2	SD
1	nat	1.000		1.000	
	f1	1.121	0.028	1.076	0.022
	f2	1.064	0.018	1.238	0.029
	f3	1.714	0.039	1.475	0.027
2	nat	1.000		1.000	
	f1	1.182	0.054	0.988	0.042
	f2	1.515	0.078	1.084	0.035
	f3	2.418	0.104	1.073	0.036
3	nat	1.000		1.000	
	f1	2.421	0.057	1.262	0.096
	f2	4.294	0.486	1.192	0.107
	f3	7.891	0.131	1.503	0.075
4	nat	1.000		1.000	
	f1	0.989	0.020	1.063	0.109
	f2	1.287	0.027	1.346	0.077
	f3	2.038	0.042	1.427	0.069
5	nat	1.000		1.000	
	f1	1.087	0.018	1.007	0.009
	f2	1.727	0.099	1.131	0.010
	f3	3.280	0.079	1.254	0.011
6	nat	1.000		1.000	
	f1	1.011	0.038	1.361	0.052
	f2	1.212	0.043	1.428	0.043
	f3	2.034	0.073	1.893	0.093
FE	nat	1.000		1.000	
	f1	1.153		1.120	
	f2	1.402		1.302	
	f3	2.168		1.669	

nat = Natural tooth; f = facial; FE = finite element.

gauges were plotted in the form of a relative value given by the equation shown in Figure 6.

Compliance was defined as strain/load. The standard error of the relative compliance was based on an approximation called “the delta method.”¹⁶ The relative local compliance of G1 and G2 are presented in Figure 7 and Table I for each specimen and each experimental situation. Because variation was small across repeat measurements of the same tooth in the same experimental condition, most notably small relative to between-tooth variation (Table I), statistical variations were not an issue in this experiment.

For a given specimen and experimental design, absolute local compliance was always higher at the level of G1 compared with G2, which resulted in greater maximum strain values at the concavity level. Although the responses of the teeth were different, a similar pattern may be observed, namely, a marked increase of compliance at G1, specifically when considering the third cut of enamel (total removal, situation f3), whereas G2 exhibits a moderate increase. Although the responses of G1 and G2 were similar after the first 2 cuts of enamel (f1 and f2), G1 always responded more intensively than G2 after

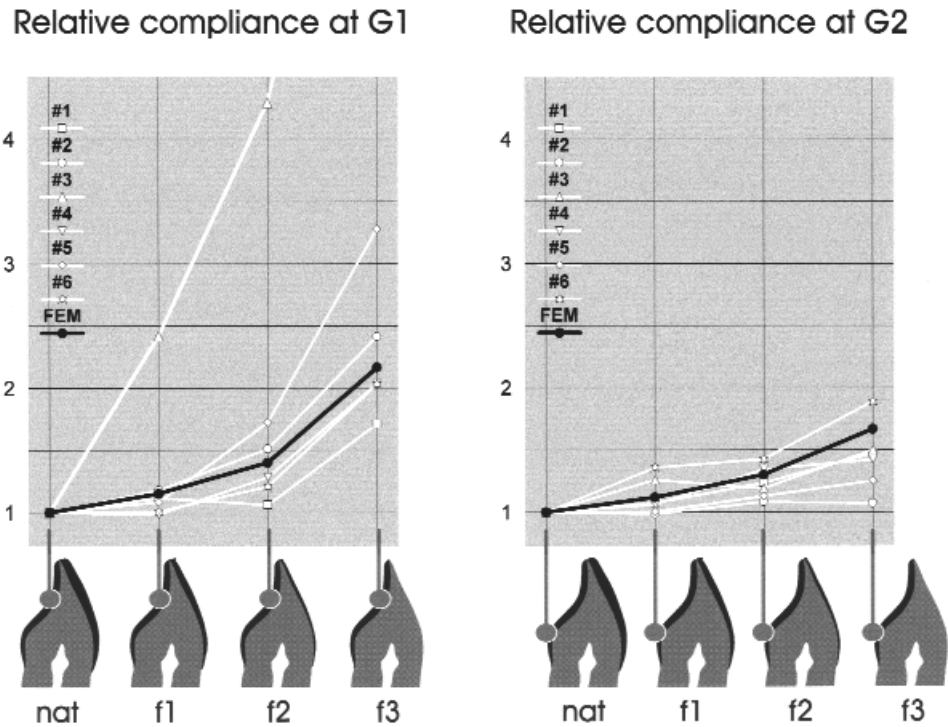


Fig. 7. Graphic representation of relative compliance given by G1 and G2 for each experimental design. To facilitate reading of chart, experimental data for each specimen (1 to 6) are linked by white line and finite element values by black line. Specimen 3 is out of scale at f3 in G1 (relative compliance = 7.9, see Table II).

the last cut (f3). Tooth specimen 4, and, to a lesser degree, specimens 1, 2, and 6, behaved similar to the finite element model. Specimens 3 and 5 exhibited a specific pattern, namely, an acute response of G1 at situation f3 (7.9× and 3.3× the original signal, respectively). The G2 signal was similar for all specimens.

Displacement of the load tip

Average displacement at the load tip was calculated from all specimens and all experimental designs together, and yielded an average value of 123 ± 37 μm. The same calculation was performed with the finite element and yielded 114 ± 22 μm displacement of the load node in the x-axis. The measurement of displacement with the current experimental apparatus may not have been sensitive enough to detect differences between the experimental designs because the results sometimes exhibited higher values before the removal of enamel.

Stress distributions

Both enamel and dentin are brittle materials that present a higher strength in compression than in tension. The strength differential effect (SDE), the ratio between compressive strength and tensile strength, has been incorporated in a failure criterion for the brittle type of materials: the modified Von Mises criterion

(mVM).¹⁷ Figure 8 illustrates stress distribution throughout the maxillary incisor section with the mVM. Significant stress concentrations are detectable on the palatal side, especially in the palatal fossa. On the opposite side, the facial half of the tooth does not show harmful stresses. It is also appropriate to analyze stresses in a direction for which the x and y components of stresses will display their maximum values. The resultant analysis (Figs. 9 and 10) outlines the principal stresses in the form of areas of compression and tension. The original tooth (Fig. 9) is separated into 2 distinct areas when subjected to a palatal load: The palatal half of the tooth exhibited positive values, namely, tensile stresses, whereas the facial half of the tooth displayed compressive stresses. Figure 10 illustrates the dramatic effect of the removal of facial enamel (condition f3) on the tensile stress distribution throughout the remaining palatal enamel. On the facial aspect, the low elastic modulus of dentin is responsible for a redistribution of compressive stresses.

The surface tangential analysis of stress is plotted in Figure 11 for each experimental design. Plot patterns were similar for all test conditions: The values are always positive on the palatal surface (maximum tensile stress in condition f3, 272 MPa), except in the area of the load point where, as expected, it is highly negative.

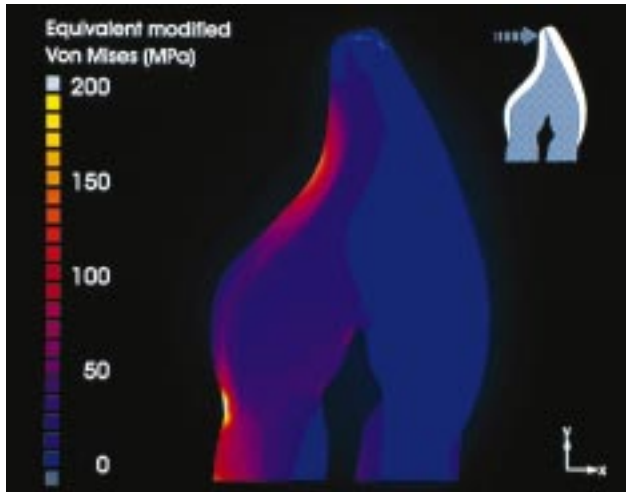


Fig. 8. Stress distribution (modified Von Mises) on natural tooth (nat) loaded horizontally with 50 N on incisal edge. Surface stress concentrations are detectable in palatal fossa and in cervical area. Facial half of tooth does not present harmful stresses.

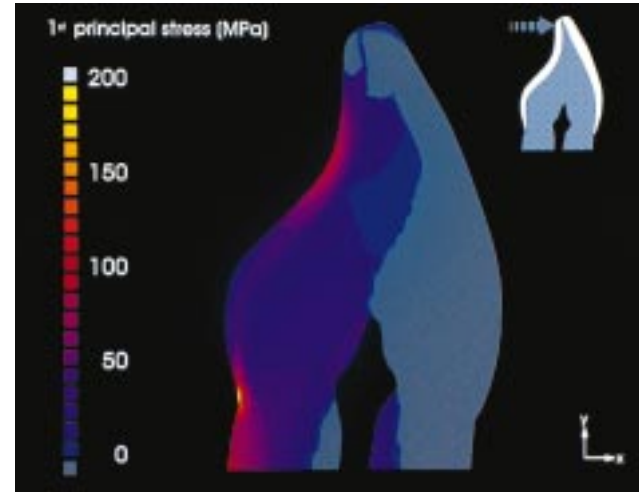


Fig. 9. First principal stresses in natural tooth (nat) loaded horizontally with 50 N on incisal edge. Negative values of stress appears in gray and delineate area of compressive stresses. Color shadings indicate different levels of tensile stresses.

On the other hand, the values are always negative on the facial surface (maximum compressive stress in condition f2, 153 MPa), except for the most incisal part of the tooth. Although palatal tensile stresses are higher in absolute than compressive facial stresses, there is a relative symmetry in the pattern of these between palatal and facial (“mirror image”), as Figure 11 shows 3 distinct areas:

1. Zone I (cervical area): An acute stress concentration peak takes place specifically at the DEJ. For either palatal or facial sides, this peak disappears when enamel is completely removed on the corresponding surface (f3 for facial, p3 for palatal).

2. Zone II (middle portion of anatomic crown): This area exhibits the lowest levels of stress, especially in highly curved palatal cingulum.

3. Zone III (incisal half of anatomic crown): In contrast with zone II, this part features another maximum stress area together with the cervical peak.

Conditions f1-f3. When enamel was removed in the facial surface, no major changes were observed in the palatal area, unless the full thickness of facial enamel was eliminated (f3). Even in that test condition, zone III was highly affected alone, whereas zone II showed almost no changes. On the facial surface, the thinned enamel concentrated highly compressive stresses. Even zone II was significantly modified (f2). Release of the facial zone II is obvious in f3, whereas palatal zone III received the highest tensile forces. Progressive migration of the DEJ peak may be observed in the facial cervical area when successively comparing nat, f1, and f2 because the removal of enamel in this area leads to the

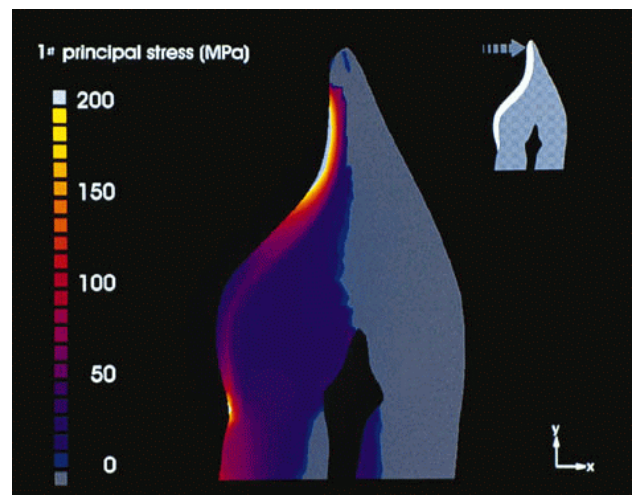


Fig. 10. First principal stresses after removal of facial enamel (condition f3). Significant increase of tensile stresses have occurred in palatal fossa, while on facial aspect, compressive stresses have been redistributed in strained dentin.

loss of the most apical elements of enamel and the subsequent incisal displacement of the DEJ.

Conditions p1-p3. The changes described previously were observed in a reversed pattern. This time, stresses were concentrated in the thinned palatal enamel (p2) and released with the total removal of the palatal enamel (p3), whereas facial zone III, and to a certain degree zone II, received the highest compressive forces. Thinning the palatal enamel (p1, p2)

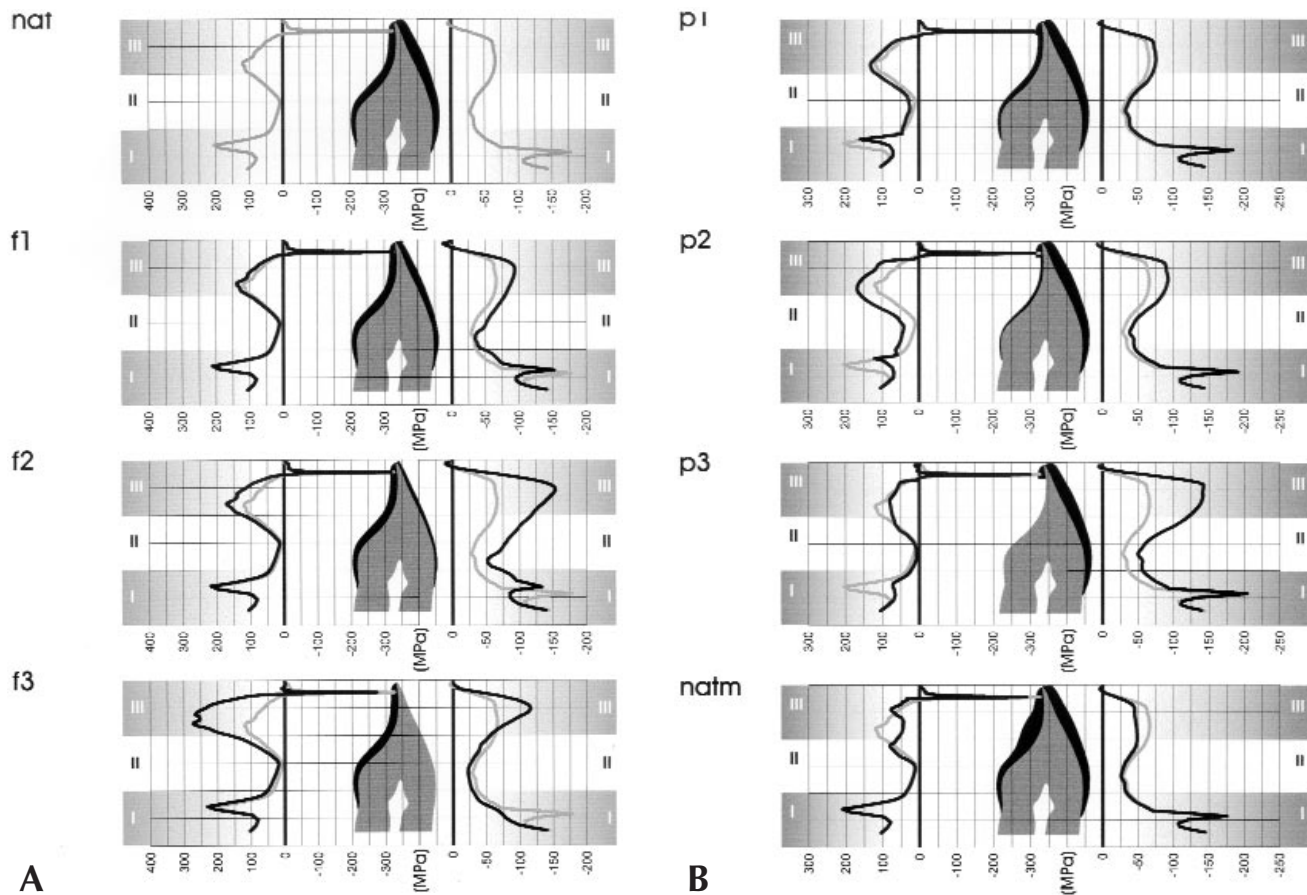


Fig. 11. Graphic representation of surface tangential stresses in MPa for each experimental design (black line). Original stress distribution of nat (gray line) is always reported as reference.

affected both palatal and facial surfaces almost symmetrically and homogeneously, whereas thinning facial enamel (f1, f2) mostly modified the stress distribution on the facial surface. However, the highest concentrations of stress were generated on either palatal or facial side after the integral removal of enamel on the opposite side.

Condition natm. The modified incisor with thickened palatal enamel displayed the lowest surface stresses in zone III, even lower than the original tooth. Modification of the palatal surface similarly affected both palatal and facial surfaces, and thus created a local drop of stress in both palatal and facial zones III. Two small peaks subsisted in the palatal surface and corresponded to concave areas delimitating the thickened enamel.

DISCUSSION

Stress distribution in natural teeth is determined by geometry and hard tissue arrangement. Finite element simulation, used to assess this complex field, was validated in this study by experimental strain gauge measurements. In a so-called “hybrid numerical–experi-

mental” approach, results of finite element analysis were also used to select the most appropriate position on the tooth surface for strain gauges in the experimental validation. Surface locations indicated by finite element analysis as the most and the least responding areas were chosen to attach the strain gauges (G1 and G2 at the palatal fossa and palatal cingulum, respectively). Experimental and numerical results revealed good correlation for both the displacement at the load point and the local compliance at the strain gauge locations. Differences observed in Figure 7 between the relative compliances of specimens 1, 2, 4, and 6 may be explained by the differences in the structure of each tooth and in the difficulty in standardizing the reduction of enamel. The higher strain responses for tooth specimens 3 and 5 (f1, f2, f3) may be attributed to enamel crack propagation under strain gauge G1, affecting its signal.

A closer examination of these specimens confirmed that the strain gauge was traversed by a horizontal flaw (Fig. 12). No such enamel cracking was observed at the level of G2, for which the signal was consistent for all



Fig. 12. Photomicrograph of tooth specimen 3 (original magnification, $\times 3$) under transillumination, at end of trial. Multiple cracks are visible on palatal surface. One of these has propagated mesiodistally under strain gauge G1, explaining unusual and extremely intense signal given by this gauge (see Fig. 7).

specimens. The effect of enamel cracks can be simulated in finite element by detaching 1 or several rows of nodes in the area of G1. In Figures 13 and 14, similar to the enamel cracks that may have been present from the start in our experimental specimens, we assumed some existing cracks in our numerical model. The resultant mVM strains and stresses are presented for 1 and 3 enamel cracks, respectively. Stress in the enamel is redistributed around the crack through the DEJ, which creates a stress concentration at the crack tip and relieves the surface strain around the crack. The surface tangential strain of the single cracked tooth was calculated for the conditions nat, f1, f2, and f3. All values were negative for G1 and all were positive for G2. Figure 15 illustrates these local compliances (surface strains at G1 and G2) for both uncracked and single cracked tooth. For cracked enamel, surface strain at G1 is reversed (compressive strain) and reduced in its absolute value. It is likely that the intense signal given at G1 for specimens 3 and 5 does not depict the real strain of the enamel surface, rather it measures the crack opening.

After the experiments, most specimens displayed multiple enamel cracks in the palatal surface, mainly in the incisal third and the palatal concavity. Enamel is a brittle material and, as a result, it is difficult to find mature intact specimens. Thus, enamel cracks can be considered a realistic enamel property. Our study was not a fracture mechanics study, and therefore crack propagation versus load was not recorded. Cracks that were observed may have been there from the start of the experiment and may have propagated during loading (while adjusting the sample setup), or extended between consecutive experiments because of preparations. Modeling of crack initiation/propagation is pos-

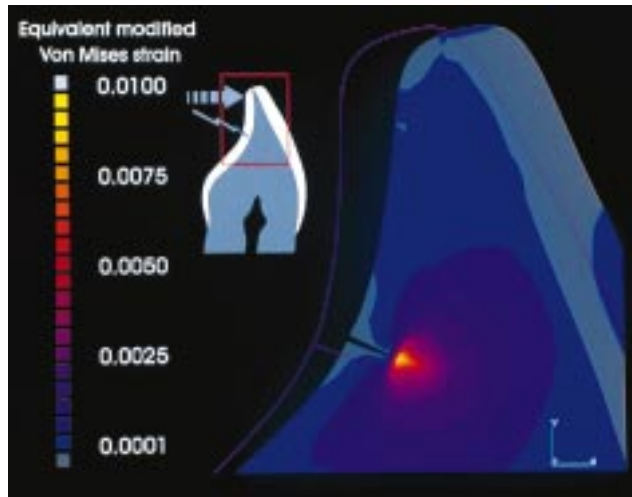


Fig. 13. Detailed view of strain distribution (modified Von Mises) in palatal fossa of cracked natural tooth loaded horizontally with 50 N on incisal edge (purple line delineates original contour of tooth, factor $\times 7$ was applied to deformation of tooth). Single crack was modeled in full thickness of enamel. Negative values of strain appear in gray in enamel surrounding flaw, indicating compressive forces at this level. Strain gauge bonded in this area would give highly positive signal by measuring crack opening.

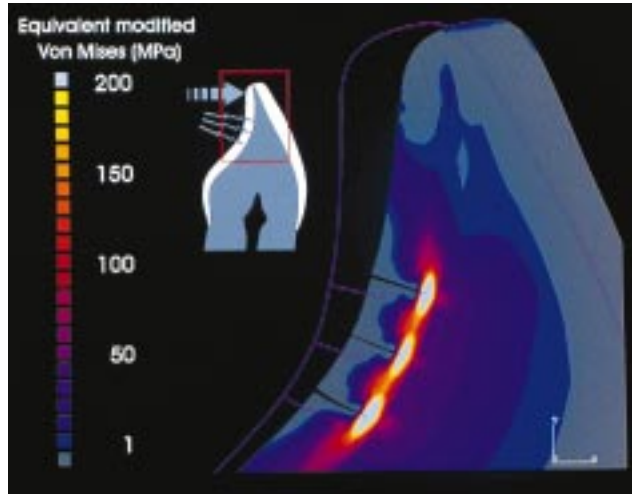


Fig. 14. Detailed view of stress distribution (modified Von Mises) in palatal fossa of cracked natural tooth loaded horizontally with 50 N on incisal edge ($\times 7$ deformation factor). Multiple cracks were modeled in full thickness of enamel. Enamel surrounding flaws is totally quiescent with regard to tensile forces.

sible by finite element modeling.⁹ However, the aim of this study was concerned with the overall stiffness behavior and the role of enamel/dentin distribution.

For all experimental designs, the compliance recorded in the palatal concavity was higher than the compli-

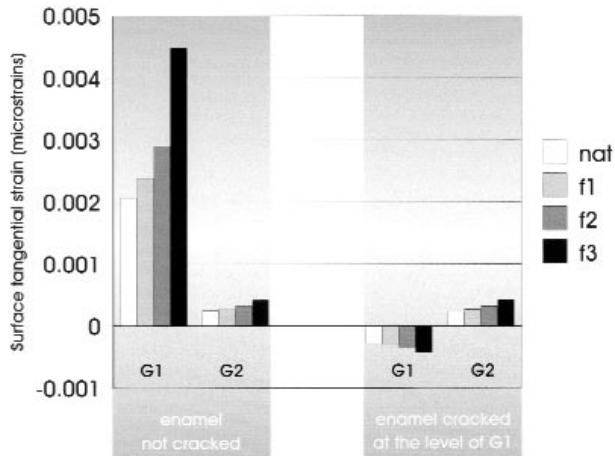


Fig. 15. Graphic representation of absolute compliance given by G1 and G2 for 2 finite element designs of intact natural tooth (uncracked and single cracked at level of G1).

ance measured on the cingulum. One may argue whether the fact that G1 was located closer to the load point logically yielded an increased signal. In the light of the data provided by the modified natural tooth (natm finite element group), such an explanation is inadequate. In this specific situation, the calculated stress in the area of G1 clearly dropped (Fig. 11) because of a change of geometry and enamel thickness. Furthermore, low stress levels were found in surfaces of maximum convex curvature, namely, the cingulum and cervical portions of the facial surface. Therefore it is concluded that convex surfaces with thick enamel raise less concentrated stresses than concave areas, which tend to concentrate stresses. Data obtained from the natm design support this observation. The residual concavities delimiting the area of thickened enamel exhibit higher tensile stresses in zone III.

The modified contour simulated in the natm design might be assumed to be the contour of an incisor in the proximal aspect of the tooth (Fig. 16) or in the presence of vertical lobes extending from the cingulum. In this regard, it can be presumed that moderate stress concentrations would occur on the totally convex palatal surfaces, such as that found on canines. Canines also present curvilinear facial surfaces that may better withstand compressive forces. An irregular surface anatomy, namely, the anatomy of the palatal surface of an incisor, logically yields to a different stress pattern. The lowest stress concentrations will be observed on smooth and convex areas (the cervical half of the crown for both palatal and facial surfaces).

Along with surface geometry, the thickness of enamel had a significant effect on stress distribution. This was evident in both finite element (group f3) and strain gauge analyses (response at G1) when the full thickness

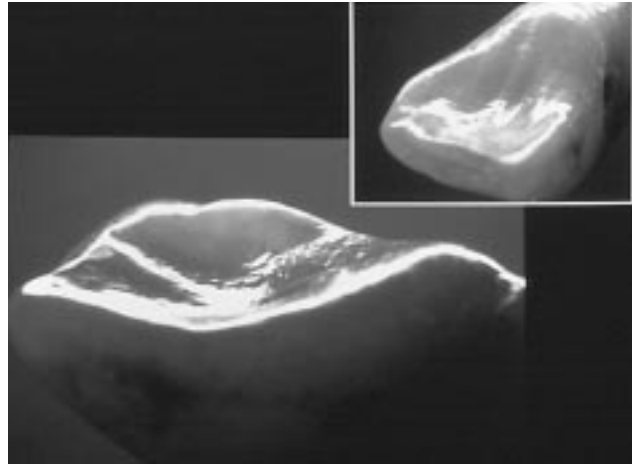


Fig. 16. Proximal view of natural incisor. Modified finite element model (natm design) reproduced prominent distal crest of tooth. This typical aspect of incisor contributes to improve stress distribution along palatal surface.

of enamel was removed from 1 side of the tooth. Consequently, the opposite side demonstrated a remarkable increase in compressive or tensile forces, especially in zones II and III. Moreover, total removal of enamel did not affect the cervical part of the tooth that remained quiescent in both finite element and strain gauge analysis (G2). A redistribution of stress from facial surface to palatal surface was noted (Fig. 11, f2 and f3). In other words, the compressive facial stress of zone II in f2 is shifted into a palatal tensile stress of zone III in f3. The same phenomenon occurs when palatal enamel is removed, leading to a translocation of higher stress from palatal in p2 to facial in p3. The transfer is more homogeneous in the last situation. Removal of enamel on 1 side affected the stress distribution at both sides of the tooth. Thus, enamel is instrumental in the way stresses are distributed in a tooth structure and it may be conceptualized as a regulator in the balance of stresses. Addition of enamel in the natm design discloses a seemingly better balance and stress distribution. In this situation, both palatal and facial curves are almost perfect “mirror” images. Small stress peaks still reveal the palatal concavities, but one may anticipate again what would be the stress pattern of a canine with its accentuated biconvex contour. When considered in the buccolingual section, such a tooth displays an almost perfect convex design that leads to a very favorable mechanical configuration, as is discussed previously. It may be concluded that the presence of an adequate enamel thickness is mandatory, not only for biologic purposes (such as wear resistance, protective cover for dentin) but also for the biomechanical balance of the tooth. Furthermore, it can be assumed that both shape and composition form an inseparable complex that determines the biomechanical behavior of a tooth.

Although the loading condition was chosen to reflect a realistic situation, it should be emphasized that the conclusions are based on only this 1 loading condition. However, conclusions regarding the effect of shape (convex vs concave) and composition (enamel-dentin distribution) are universal and do not depend on the exact load direction or magnitude. This statement has been confirmed by reversing the load direction.

Several clinical perspectives can be outlined from our study. When enamel is cut to access a proximal decay or for a veneer, the future restoration must restore the original compliance of the tooth to avoid a shift in stress distribution, which may lead to increased stress concentrations and enamel yield. Composite restorations have not demonstrated the ability to restore the original stiffness of the tooth completely.^{5,6} Similar observations were made on posterior teeth when preparing an MOD cavity.¹⁸ Only replacement of enamel with a material possessing a similar elastic modulus would be able to restore the so-called "biomechanical balance" of the original tooth. Cracks encountered during the experimental portion of this study may have been the consequence of an "unbalanced configuration" created by enamel loss. Clinically, similar full thickness enamel cracks are observed when crown rigidity is affected. Finally, the finite element analysis showed concentration of stress at the enamel-dentin junction. It is noted that cervical abfraction can be observed in the same area.¹⁹ However, the finite element model was not designed to focus on this specific transition zone that would require a more detailed model definition in the concerned areas.

CONCLUSIONS

Stress and strain measurements made on both extracted teeth and numerical models demonstrated that stress distribution within natural teeth is determined by geometry and hard tissue arrangement. On the basis of the results of this simulation study, the following conclusions were drawn:

1. For an incisor, a sufficient and uniform enamel thickness is essential to the "balance" of stresses between the facial and palatal surfaces. With an incisal palatal load, the facial half of the tooth is mainly subjected to compressive stresses, whereas the entire palatal portion of the tooth is exposed to tensile stresses.

2. The concave palatal surface provides the incisor with its cutting ability. However, enamel in the palatal concavity exhibited a high crack propensity due to elevated tensile stresses developed in this specific area under functional load.

3. The extremely convex cingulum, the facial cervical third of enamel, and the palatal proximal ridges represent quiescent areas with regard to stress and strain.

4. High stress concentrations were detectable when enamel was worn down or removed from the facial sur-

face. Consequently, the replacement of enamel should be performed by using materials with properties similar to enamel to restore the original biomechanical behavior of the tooth.

We express our gratitude to Prof Maria Pintado (Minnesota Dental Research Center for Biomaterials and Biomechanics) for her precious help and technical support and Dr James Hodges (Minnesota Oral Health Clinical Research Center, NIH/NIDR P30-DE09737) for the analysis of data presented in this report.

REFERENCES

- Morin DL, Douglas WH, Cross M, De Long R. Biophysical stress analysis of restored teeth: experimental strain measurement. *Dent Mater* 1988;4:41-8.
- Morin DL, Cross M, Voller VR, Douglas WH, De Long R. Biophysical stress analysis of restored teeth: modelling and analysis. *Dent Mater* 1988;4:77-84.
- Kraus BS, Jordan RE, Abrams L. Histology of the teeth and their investing structures. In: *Dental anatomy and occlusion*. Baltimore: Williams and Wilkins; 1969. p. 135.
- Lin CP, Douglas WH. Structure-property relations and crack resistance at the bovine dentin-enamel junction. *J Dent Res* 1994;73:1072-8.
- Douglas WH. The esthetic motif in research and clinical practice. *Quintessence Int* 1989;20:739-45.
- Reeh ES, Ross GK. Tooth stiffness with composite veneers: a strain gauge and finite element evaluation. *Dent Mater* 1994;10:247-52.
- Koroth TW, Versluis A. Modeling the mechanical behavior of the jaws and their related structures by finite element (FE) analysis. *Crit Rev Oral Biol Med* 1997;8:90-104.
- Lin CP, Douglas WH. Failure mechanisms at the human dentin-resin interface: a fracture mechanics approach. *J Biomech* 1994;27:1037-47.
- Versluis A, Tantbirojn D, Douglas WH. Why do shear bond tests pull out dentin? *J Dent Res* 1997;76:1298-307.
- Kinney JH, Balooch M, Marshall SJ, Marshall GW Jr, Weihs TP. Hardness and Young's modulus of human peritubular and intertubular dentine. *Arch Oral Biol* 1996;41:9-13.
- Kinney JH, Balooch M, Marshall SJ, Marshall GW Jr, Weihs TP. Atomic force microscope measurements of the hardness and elasticity of peritubular and intertubular human dentin. *J Biomech Eng* 1996;118:133-5.
- Versluis A, Douglas WH, Cross M, Sakaguchi RL. Does an incremental filling technique reduce polymerization shrinkage? *J Dent Res* 1996;75:871-8.
- Watts DC, el Mowafy OM, Grant AA. Temperature-dependence of compressive properties of human dentin. *J Dent Res* 1987;66:29-32.
- Craig RG. *Restorative dental materials*. 6th ed. St Louis: CV Mosby; 1980. p. 76.
- Gere JM, Timoshenko SP. Analysis of stress and strain. In: *Mechanics of materials*. 3rd ed. Boston: PWS Publishing; 1990. p. 378-460.
- Rao CR. *Linear statistical inference and its applications*. 2nd ed. New York: JW Wiley; 1973. Section 6a.2.
- De Groot R, Peters MC, De Haan YM, Dop GJ, Plasschaert AJ. Failure stress criteria for composite resin. *J Dent Res* 1987;66:1748-52.
- Morin D, De Long R, Douglas WH. Cusp reinforcement by the acid-etch technique. *J Dent Res* 1984;63:1075-8.
- Grippio JO. Abfractions: a new classification of hard tissue lesions of teeth. *J Esthet Dent* 1991;3:14-9.

Reprint requests to:

DR PASCAL MAGNE
MINNESOTA DENTAL RESEARCH CENTER FOR BIOMATERIALS AND BIOMECHANICS
SCHOOL OF DENTISTRY
UNIVERSITY OF MINNESOTA
515 DELAWARE ST SE
MINNEAPOLIS, MN 55455-0329
FAX: (612)626-1484
E-MAIL: pascal@web.dent.umn.edu

Copyright © 1999 by The Editorial Council of *The Journal of Prosthetic Dentistry*.

0022-3913/99/\$8.00 + 0. 10/1/95500